Supporting Information

ARTICLE TITLE

An alternative enzyme protection assay to overcome the drawbacks of gentamicin protection assay for measuring entry and intracellular survival of Staphylococci

RUNNING TITLE

Precise quantification of intracellular bacteria

AUTHORS

Jin-Hahn Kim[1, §], Akhilesh Kumar Chaurasia[1, §], Nayab Batool[1], Kwan Soo Ko[1], and Kyeong Kyu Kim[1, 2] *

[1]Department of Molecular Cell Biology, Institute for Antimicrobial Resistance Research and Therapeutics, Sungkyunkwan University School of Medicine, Suwon 16419, Korea

[2]Samsung Biomedical Research Institute, Samsung Advanced Institute for Health Sciences and Technology, Samsung Medical Center, Sungkyunkwan University School of Medicine, Seoul 06351, Korea

[§]These authors contributed equally to this work

*To whom all correspondence should be addressed:

Tel: 82-31-299-6136

Fax: 82-31-299-6159

E-mail: kyeongkyu@skku.edu

Contents:

A. Supplementary figures

extracellular killing of *S. aureus* infected into RAW264.7 cells

14. **Supplementary Figure S14.** Snapshot of video V2 showing lysostaphin-mediated killing of extracellular *S. aureus* infected into RAW264.7 cells

B. Supplementary videos

1. **Supplementary Video V1.** Visualization of the gentamicin-mediated killing of extracellular and host cell surface-attached *S. aureus* for 1 h after 30-min invasion of *S. aureus* and phagocytosis by host cells
2. **Supplementary Video V2.** Visualization of the lysostaphin-mediated instantaneous killing of extracellular and host cell surface-bound *S. aureus*

C. References

A. Supplementary Figures

FIG S1

A

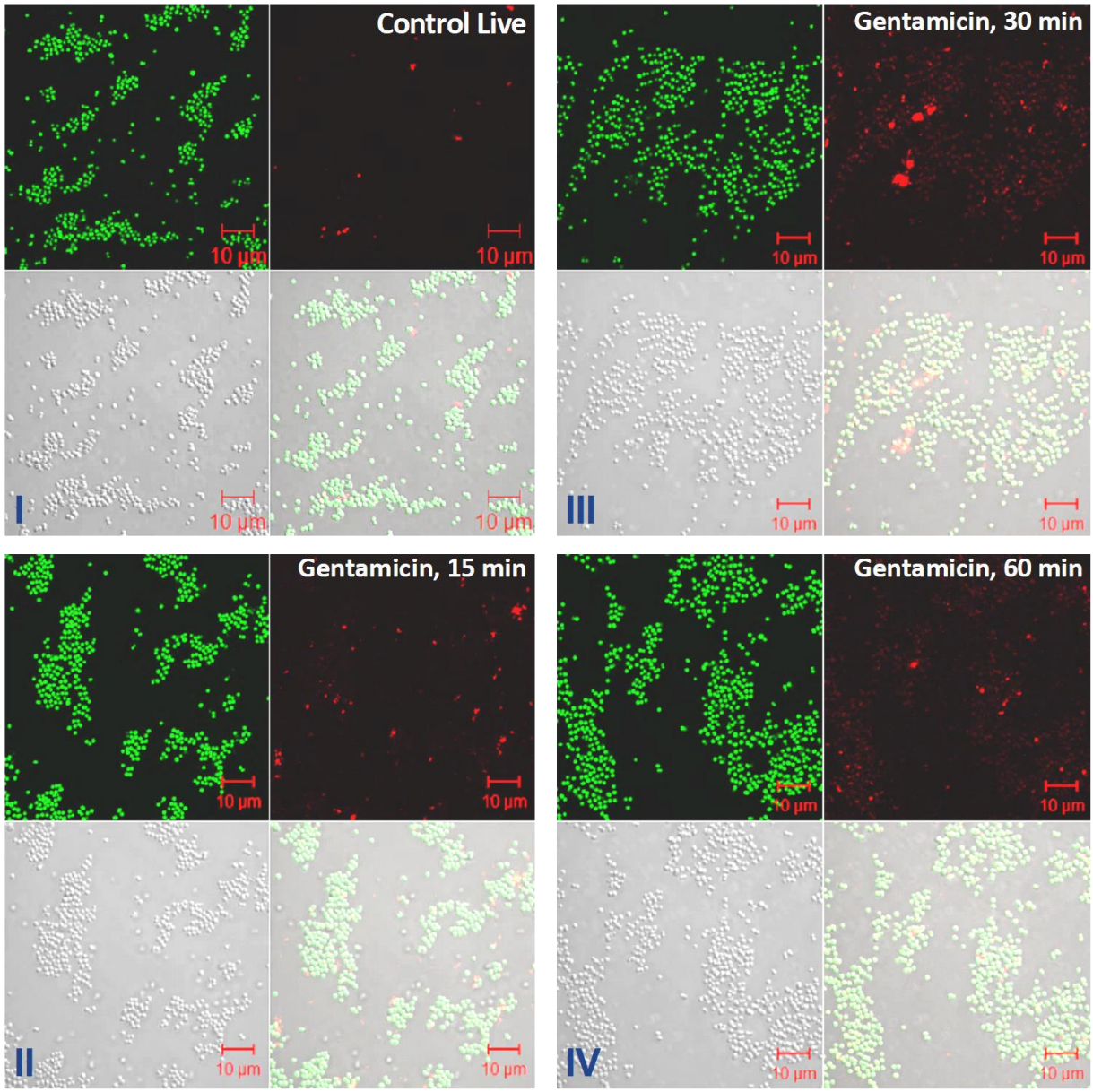

B

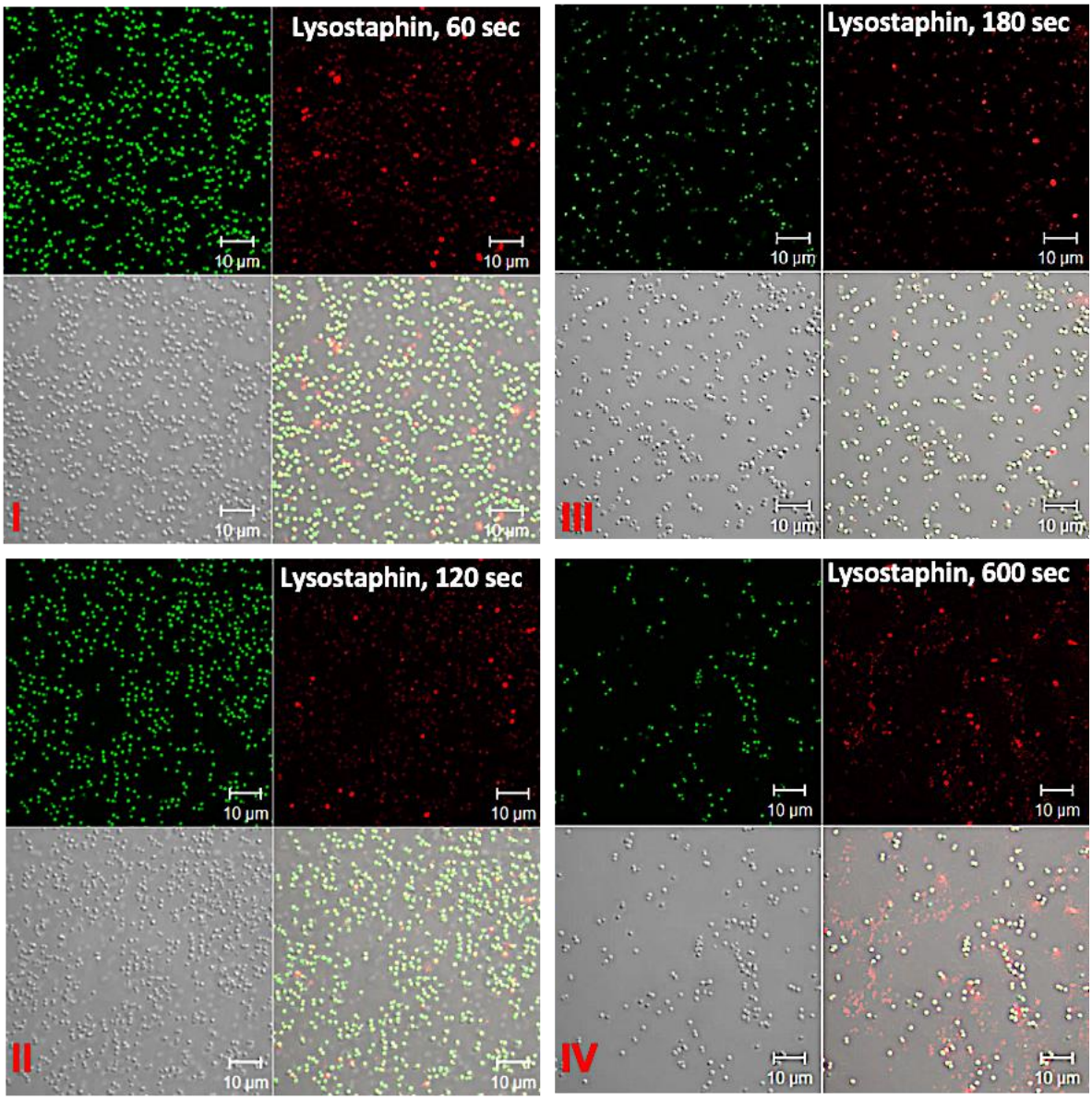

FIG S1 Qualitative assessment of gentamicin and lysostaphin-mediated killing efficiency for *S. aureus*. (A) The gentamicin-mediated killing for *S. aureus* (400 µg/ml or 840 µM for 1 h) investigated by confocal image. Confocal image (I) indicates the live cells without any treatment, while images (II-IV) depict the gentamicin-mediated killing efficiency for *S. aureus* at various time points (II) 15 min, (III) 30 min and (IV) 60 min. **(**B) The lysostaphin-mediated killing for *S. aureus* (2U or 17.6 nM for 600 sec) investigated by confocal image. Lysostaphin was treated for (I) 60, (II) 120, (III) 180, and (IV) 600 sec. Bacteria were grown in DMEM media devoid of FBS at 37°C in 5% CO_2 incubator. The BacLight bacterial viability kit (L7007 LIVE/DEAD BacLight™) was used for the qualitative assessment of dead bacteria by confocal

imaging. The kit solution contains two nucleic acid fluorescent stains, SYTO9 (green fluorescence) and propidium iodide (PI, red fluorescence). Each confocal microphotograph (Fig S1A & Fig S1B) shows four panels, wherein the first shows green (SYTO9 fluorescence); the second red (PI fluorescence); the third bright-field; and the fourth the merged image of the three panels described above. Since SYTO9 is permeable to all (live and dead) bacterial cells, SYTO9 stained all bacterial cells in green fluorescence, providing the total number of bacterial counts. In contrast, propidium iodide can enter only dead bacteria with compromised/damaged membranes. Therefore, the dead bacteria with membrane damage displayed the red or orange fluorescence, the green and red fluorescence signals being mixed. Most of the *S. aureus* cells were damaged due to extremely high killing activity of lysostaphin. It is noteworthy that the amount of PI entered in the case of gentamicin mediation is lower than the case with lysostaphin mediated killing, because the killing mechanism of gentamicin is not directly through membrane damage.

FIG S2

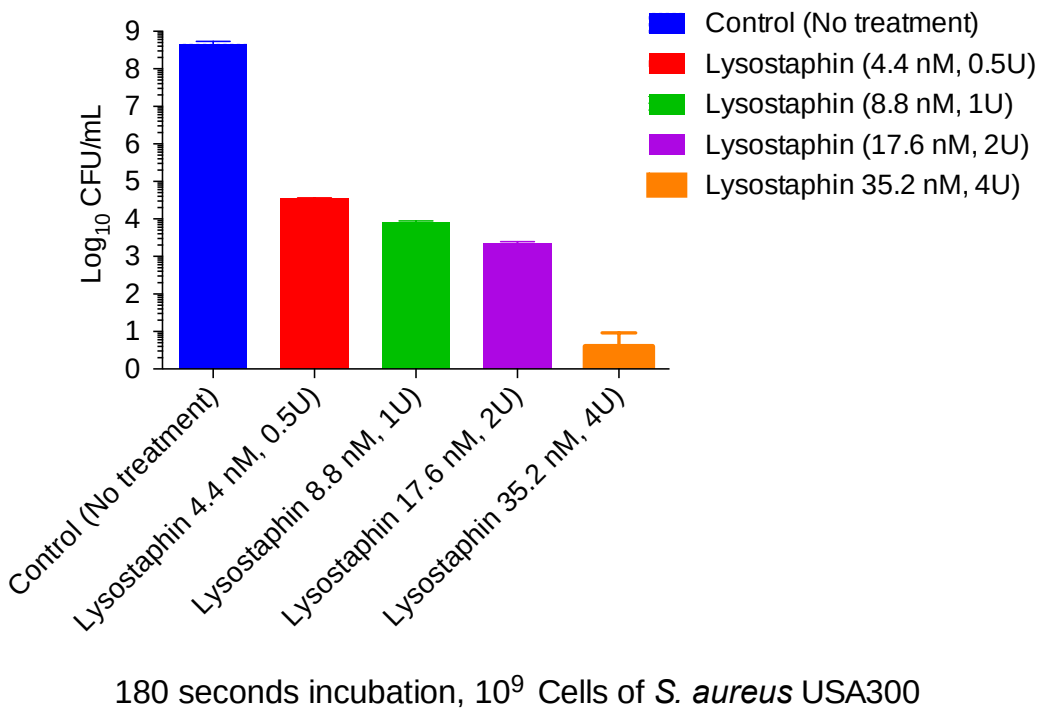

FIG S2 Killing efficiency of lysostaphin for the high-density *S. aureus*. Varying concentrations of lysostaphin (4.4 nM to 35.2 nM) were used to test the killing efficiency of lysostaphin for the high-density *S. aureus* at the fixed incubation time of 180 sec. Log phage grown *S. aureus* cells were harvested by centrifugation at 4000 rpm (3220 ×g) for 10 min at 4°C and washed once with phosphate buffer saline (PBS, pH 7.4). Then, *S. aureus* cell-suspension (OD_{600} = 1, 6 ml) was made in DMEM media devoid of FBS, and the experiment was set-up using 1 ml for each of the treatments, as shown in the figure label. The high-density *S. aureus* cells (~ 10^9), which are more likely to occur under both *in vitro* conditions at high multiplicity of infection (*moi*) experiment and under circumstances of severe infection, were killed at 4 U (35.2 nM) lysostaphin within 180 sec.

FIG S3

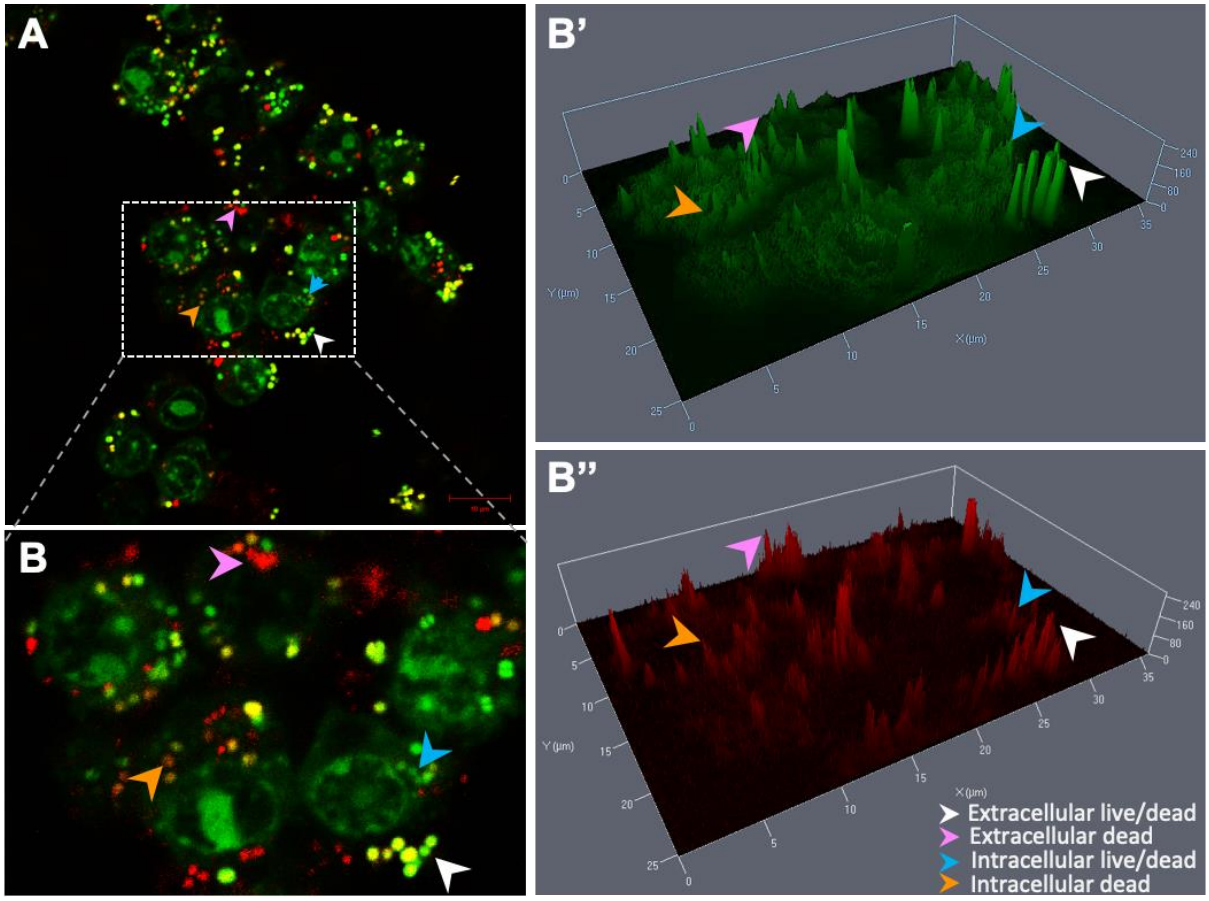

FIG S3 Confocal image analysis of gentamicin protection assay (GPA) to evaluate the extracellular and intracellular localization of *S. aureus* in mouse macrophage, RAW264.7 cells. (A) The BacLight viability-stained *S. aureus* was infected into RAW264.7 cells for 30 min, followed by gentamicin treatment (840 µM for 2h) during GPA. (B) Cropped region of Image A (B'-B"). Image B was analyzed using Zen software (ZEISS) to measure the fluorescence intensity of SYTO9 (green dot, B'), and PI (red dot, B") to evaluate the localization of *S. aureus* cells. The red dots with fluorescence intensity around 210±20 au are considered to be dead *S. aureus* cells present in extracellular space or on the host cell-surface, and those around ~120±20 au are expected to be the dead cells inside the host cells. Various color arrowheads depict the position and state of *S. aureus* cells. The white arrowhead indicates extracellular bacteria, but arrowhead in pink indicates the dead bacteria present in the host cell-surface and extracellular milieu. The sky blue and orange arrowheads show intracellular live/dead and intracellular dead bacteria, respectively. A significant number of intracellular dead *S. aureus* cells were detected in the representative image of GPA.

147 **FIG S4**

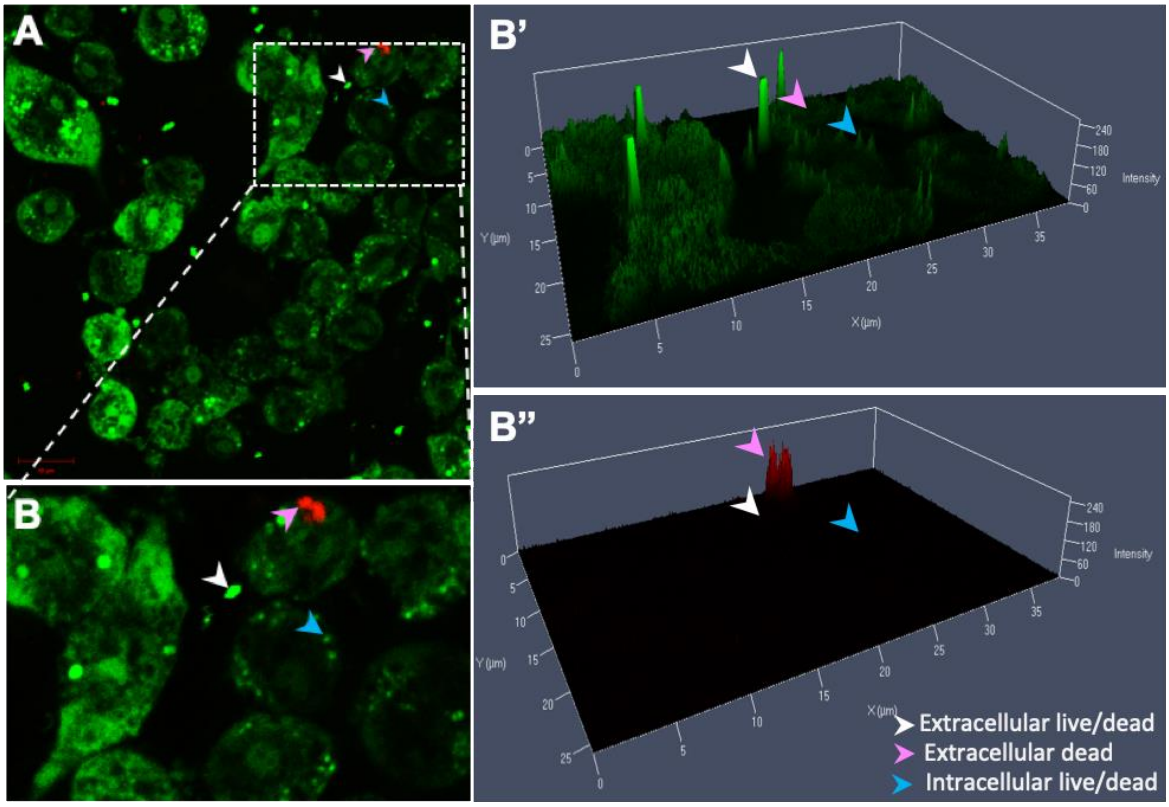

148

149 FIG S4 Analysis of enzyme protection assay (EPA) confocal image to envisage the extracellular and
150 intracellular localization of *S. aureus* in mouse macrophage, RAW264.7 cells. (A) The BacLight viability-
151 stained *S. aureus* was infected into RAW264.7 cells for 30 min, followed by lysostaphin treatment (2 U,
152 for 10 min) during EPA. (B) Cropped region of Image A (B'-B"). Image B was analyzed in the same way
153 as Fig S3B. The color arrowhead depiction is the same as indicated in Fig S3. It is noteworthy that no
154 intracellular dead *S. aureus* cells were detected in the representative image of EPA. The image analysis of
155 intracellular dead bacteria in Fig S3B" and S4B", the proportion of dead intracellular *S. aureus* in GPA
156 *versus* EPA is phenotypically evident. However, based on the counting of a 2D image (Fig. S4B"), no
157 intracellular dead *S. aureus* (PI-stained red dot) was found during EPA. Therefore, the counting of dead
158 intracellular bacteria based on image analysis is practically not possible during EPA. Nonetheless, the
159 precise CFU counting method yielded the difference between two methods (GPA *versus* EPA) in the
160 recovery of intracellular living *S. aureus* was about five times (Fig. 1D), and the CFU count varies within
161 one $\log_{10}$CFU value depending upon the time of infection (Fig. 5C).

162

FIG S5

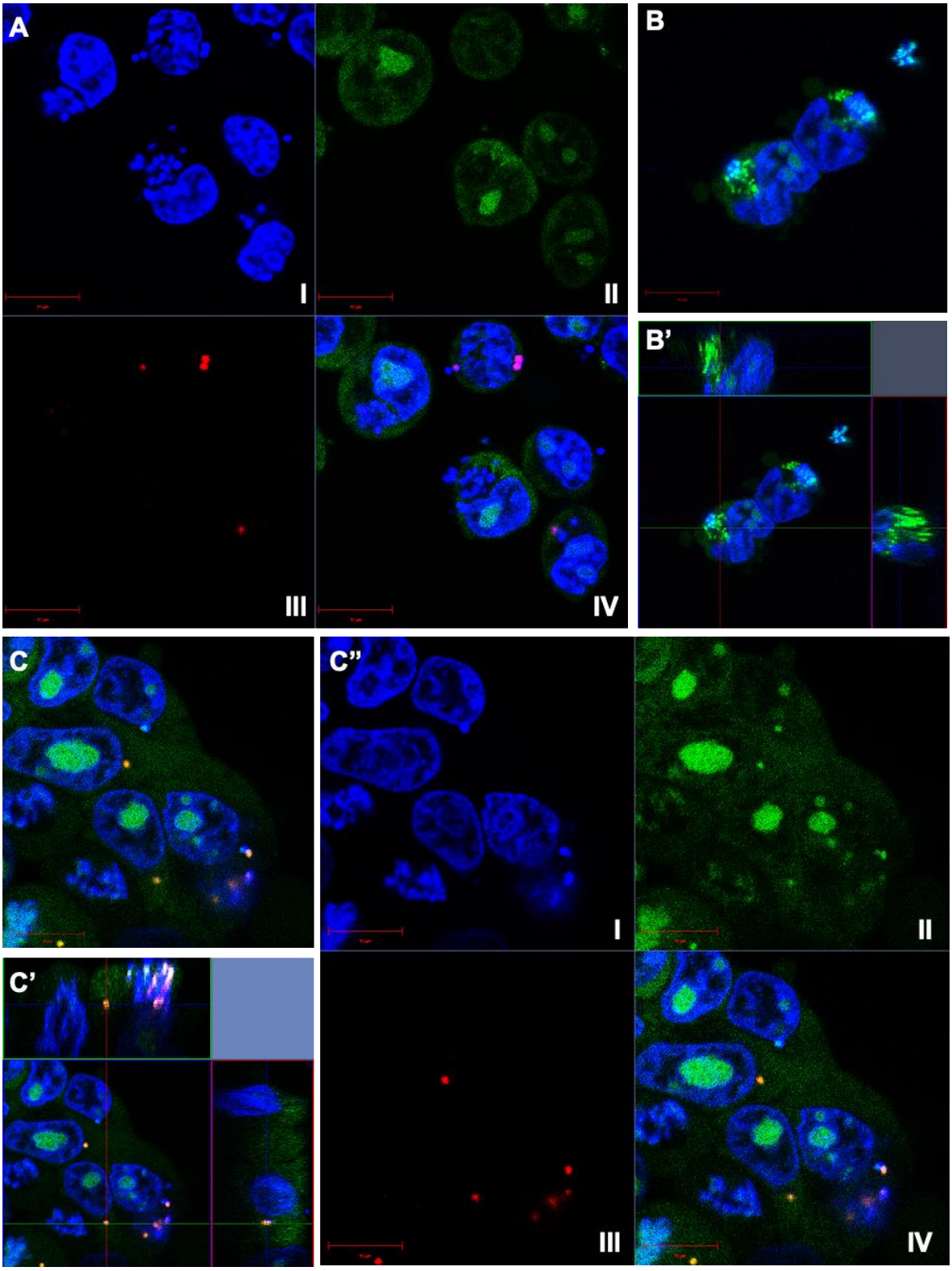

FIG S5 Qualitative confocal image analysis to confirm the intracellular killing of *S. aureus* during GPA both in mouse macrophage (RAW264.7) and human embryonic kidney (HEK293) cell lines. (A) Confocal images showing the split channel of Fig 2C, in which RAW264.7 cells infected with *S. aureus* were

subjected to GPA. Four panels show (I) the nucleus of RAW264.7 stained blue using Hoechst 33258 for live cell imaging; (II) the SYTO9 channel showing intracellular *S. aureus* and slightly greenish cellular boundary of RAW264.7, most likely due to the diffusion of SYTO9 from the LIVE/DEAD BacLight labeled *S. aureus* cells used for infection; (III) the PI-stained dead intracellular *S. aureus;* and (IV) the merged image of the aforesaid channels (I)-(III). (B-B') Live cell confocal images of the *S. aureus*-infected HEK293 cells without GPA. The center stack of Z-stack images (B) and their ortho-images (B') show the presence of intracellular *S. aureus* in HEK293 host cells. (C-C") Confocal images showing intracellular killing of *S. aureus* in nonphagocytic host HEK293 cells during GPA. (C) Two-dimensional image of the center stack of the Z-stack image shows red fluorescent *S. aureus* cells in host cells. (C') The ortho-image analysis of (C) reveals the dead intracellular *S. aureus* in HEK293. (C") The split channel images of the merged image (C') depict, (I) Hoechst 33258 stained nucleus of HEK293 cells, (II) the SYTO9 stained intracellular *S. aureus* and slightly greenish cellular boundary of HEK293 cells, (III) the PI-stained dead intracellular *S. aureus,* and (IV) the merged image of the aforesaid channels (I)-(III). The Z-stack live cell images of phagocytic RAW264.7 and nonphagocytic HEK293 with *S. aureus* infection treated with GPA showed that non-specific killing of intracellular *S. aureus* occurs in both host cells.

FIG S6

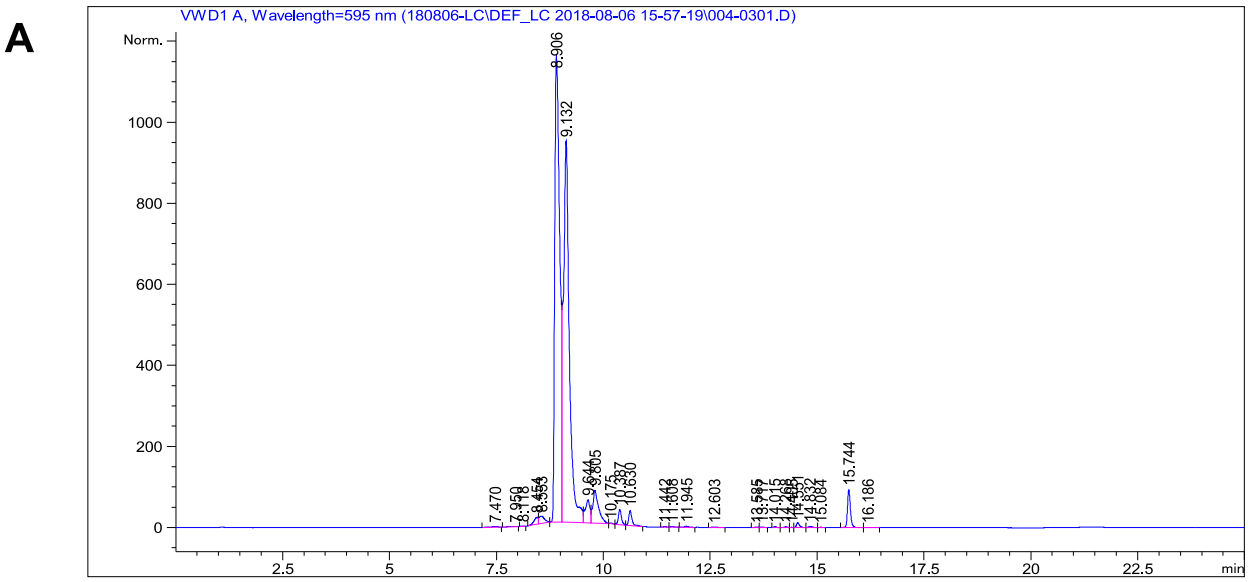

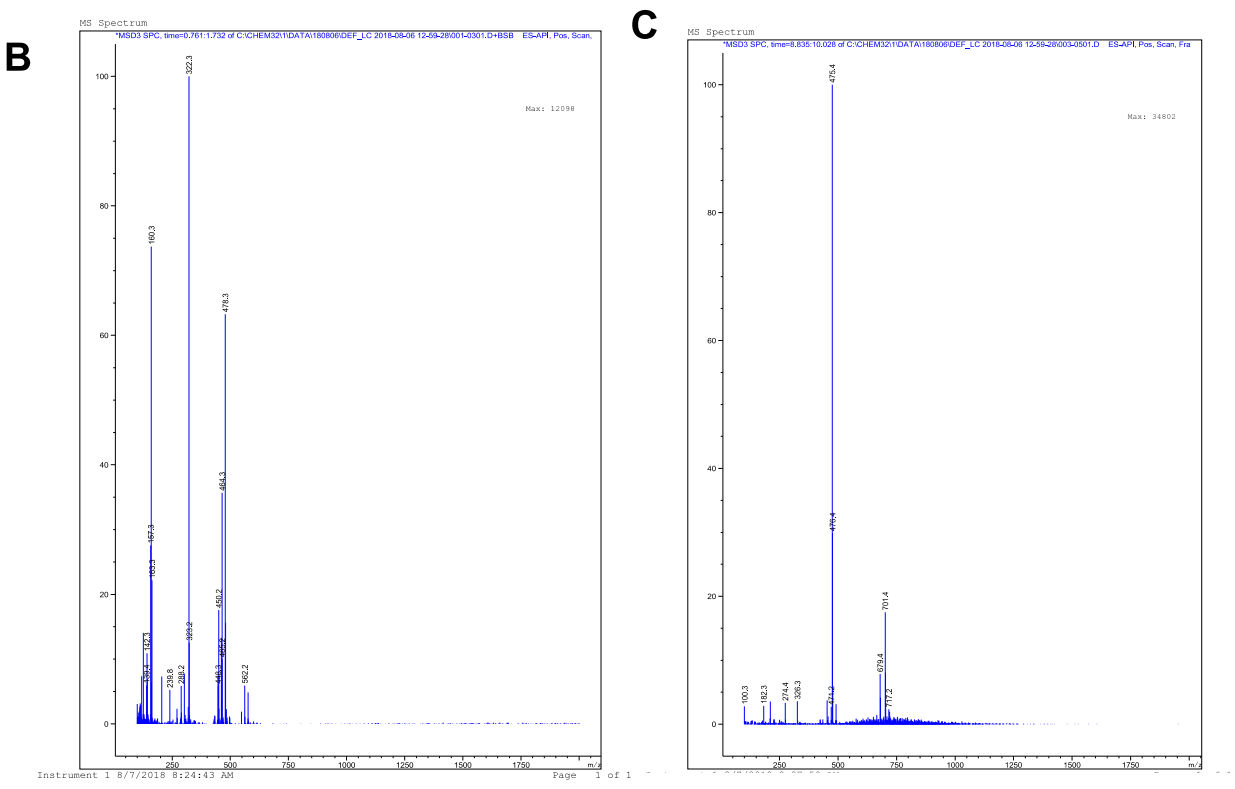

FIG S6 Conjugation of gentamicin (GT) to Texas Red-X succinimidyl ester (TR) to visualize the internalization of gentamicin-TR (GTTR) into host cells. (A) Liquid chromatographic separation of conjugated product, GTTR. (B) Mass analysis of GT. (C) Mass analysis of GTTR. The method of LC/MS for the separation of GTTR and mass analysis are performed as descried earlier (1).

FIG S7

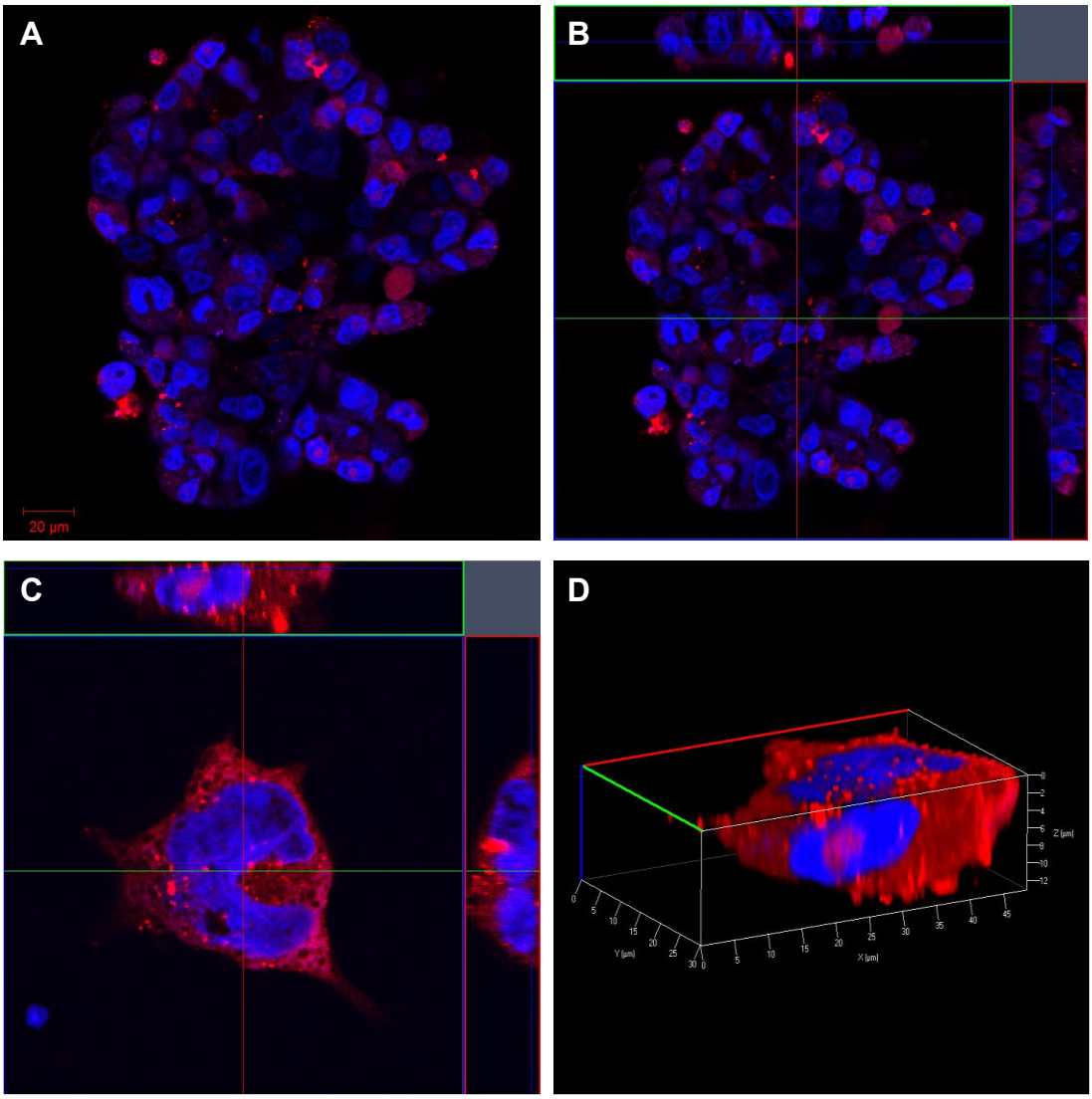

FIG S7 Visualization of gentamicin-TR (GTTR) internalization into the HEK293 cells. GTTR at 50 µg/ml was incubated with HEK293 cells for 1 h. The excess GTTR was removed and washed gently thrice with PBS (pH 7.4), followed by an addition of 2 µl of Hoechst 33258 (10 mg/ml stock) in the confocal disc, which contained 1 ml media to stain the nucleus for 10 min at 37°C in CO_2 incubator. After nuclear staining, the host cells were washed once with PBS and fixed with freshly prepared and filtered (0.22 µ) 4% paraformaldehyde. The fixed cells were washed thrice with PBS. After washing, the cells in confocal disc were overlaid with 300 µl of PBS. (A) 2D image of HEK293 cells showing GTTR red fluorescence. (B) Ortho-image of the center stack of Z-stack images of HEK293 cells showing the presence of GTTR red fluorescence in the cytosol. (C) A single enlarged cell was imaged in Z-stack. (D) The three-dimensional

model of the enlarged HEK293 cell (C) was vertically dissected as shown by a red line to analyze the internalization of GTTR. The dissected three-dimensional image showed the intracellular red fluorescence signal of GTTR which confirmed the internalization of gentamicin-TR into the HEK293 cells.

FIG S8

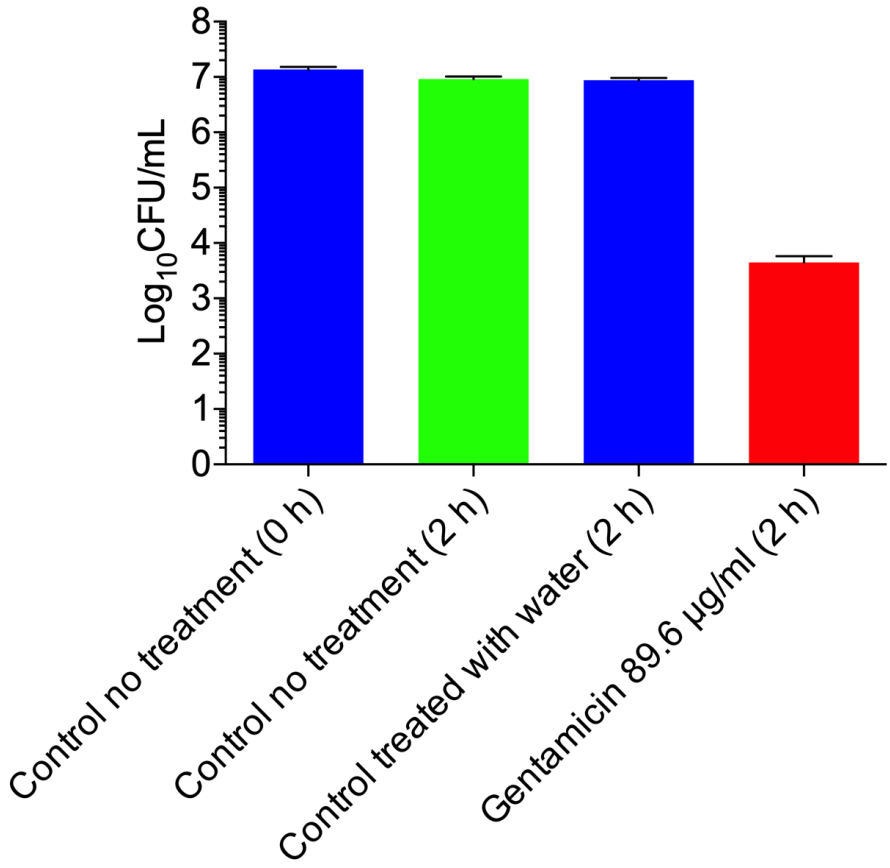

FIG S8 Bactericidal activity of the gentamicin at the concentration equivalent to the host-cell internalized gentamicin. The log phase grown *S. aureus* cells (OD_{600} equivalent 0.01 or ~1×10^7) in DMEM media devoid of FBS, were incubated without or with 89.6 µg/ml of gentamicin for 2h at 37°C in for 2 h under shaking culture conditions. The control was exposed to the equivalent volume of autoclaved water. The decrease in ~3 $\log_{10}$CFU value of *S. aureus* during the gentamicin treatment was observed. This result signified and established that the 89.6 µg/ml concentration of gentamicin could kill *S. aureus* cells under *in vitro* conditions, suggesting that the internalized gentamicin can kill *S. aureus* inside the host cells.

FIG S9

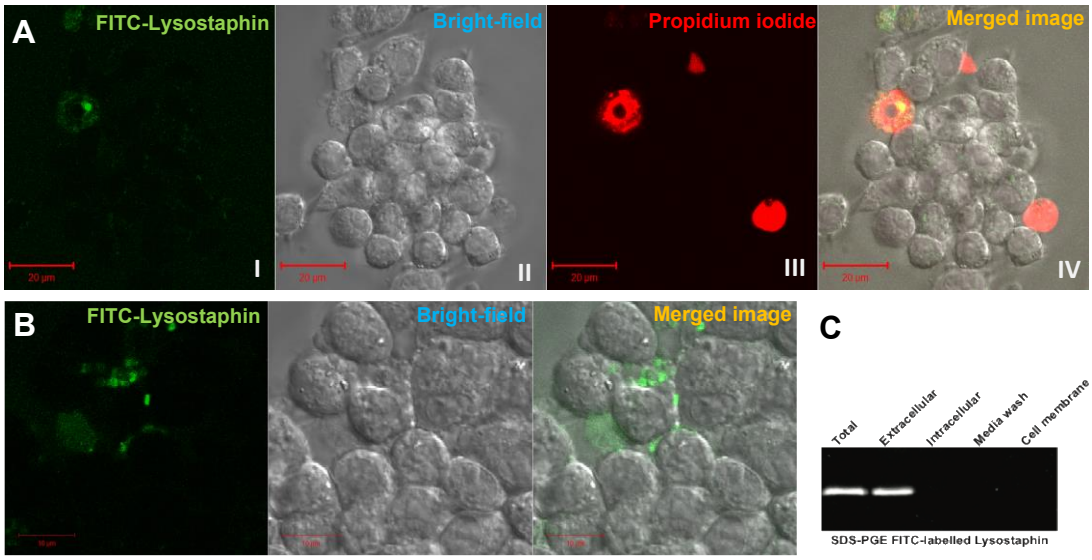

FIG S9 Assessment of the internalization of lysostaphin into host cells. (A) Live cell imaging of RAW264.7 cells treated with FITC-labeled lysostaphin. RAW264.7 cells were incubated with FITC-lysostaphin for 30 min followed by propidium iodide (PI) staining for the visualization of dead cells. The stained cells were observed using confocal laser scanning microscopy with FITC (I), DIC (II), and PI (III) filters. Panel IV shows the merged image of I-III. The FITC-labeled lysostaphin was found only in dead cells, red-stained by PI, suggesting that lysostaphin is impermeable to live cells. (B) The FITC-lysostaphin was added to RAW264.7 cells for 10 min, and then cells were immediately fixed with 4% paraformaldehyde without washing to stop the endolysosomal-network and its subsequent acidification, which raises a possibility of fluorescence quenching of FITC at acidic pH. The quenching and inability to detect FITC may result in a misinterpretation that lysostaphin could not enter into the host cells. The FITC-lysostaphin was not detected in the cytosolic space in the fixed cell images, but was localized in extracellular space and on cellular boundaries. (C) The FITC-labeled lysostaphin was applied to RAW264.7 host cells for 30 min at 37°C in 5% CO_2 incubator. Each cell lysis was fractionized and analyzed by SDS-PAGE, followed by sensitive fluorescence imaging. FITC-lysostaphin was observed only in the extracellular fraction, suggesting that lysostaphin may have: failed to internalize, or had been internalized at undetectable level, or had been proteolytically degraded by the host cell. Nonetheless, these results eliminate the possibility of any non-specific killing of internalized bacteria by lysostaphin during EPA.

FIG S10

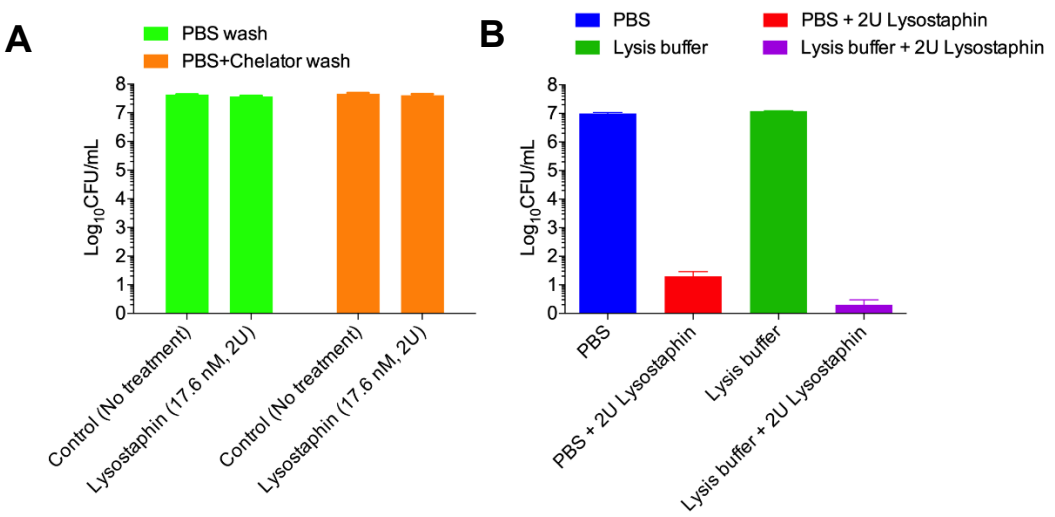

FIG S10 Effect of host cell-internalized lysostaphin on *S. aureus*. (A) The 80% confluent RAW264.7 cells (72 h) grown in DMEM media with 10% FBS was used to assess the effect of internalized lysostaphin, if any, on *S. aureus*. The utilized DMEM media was replaced with fresh DMEM media devoid of FBS before 1 h. The RAW264.7 cells were treated with buffer (control) or 2 U of lysostaphin for 30 min at 37°C with 5% CO_2. Then, used DMEM media was aspirated and the host cells- or microtitre plate surface- adhered lysostaphin was washed with PBS, or PBS with 100 µM 1,10-phenanthroline, followed by two cycles of additional gentle washing with PBS. The control and lysostaphin-treated RAW264.7 cells were collected using rubber scrapper in 1 ml PBS. The cell pellets were lysed in 1.0 ml of the lysis buffer. The 1 ml cell-free extract was used to treat log phase grown *S. aureus* cells for 2 h at 37°C in 5% CO_2 incubator. The *S. aureus* cells were diluted in PBS and plated on TSB-agar plate. No significant change in the CFU was observed between the control and lysostaphin treated cell extracts, confirming either that (1) lysostaphin could not enter or (2) was degraded proteolytically upon entry into the host cells. (B) Assessment of killing activity of lysostaphin upon exposure to mammalian cell lysis buffer (0.04% Triton X-100 in autoclaved MilliQ water). Phosphate buffer saline (PBS) and lysis buffer (988 µl) were added with 2U (2 µl) of lysostaphin. The overnight grown *S. aureus* cells were washed with PBS once. An equivalent volume (10 µl of the OD_{600} = 1) to 10^7 cells was added to PBS and lysis buffer without and with lysostaphin. In fact, the exposure of lysostaphin to the extremely low concentration of Triton X-100 (0.04%) has slightly enhanced the lysostaphin killing activity.

FIG S11

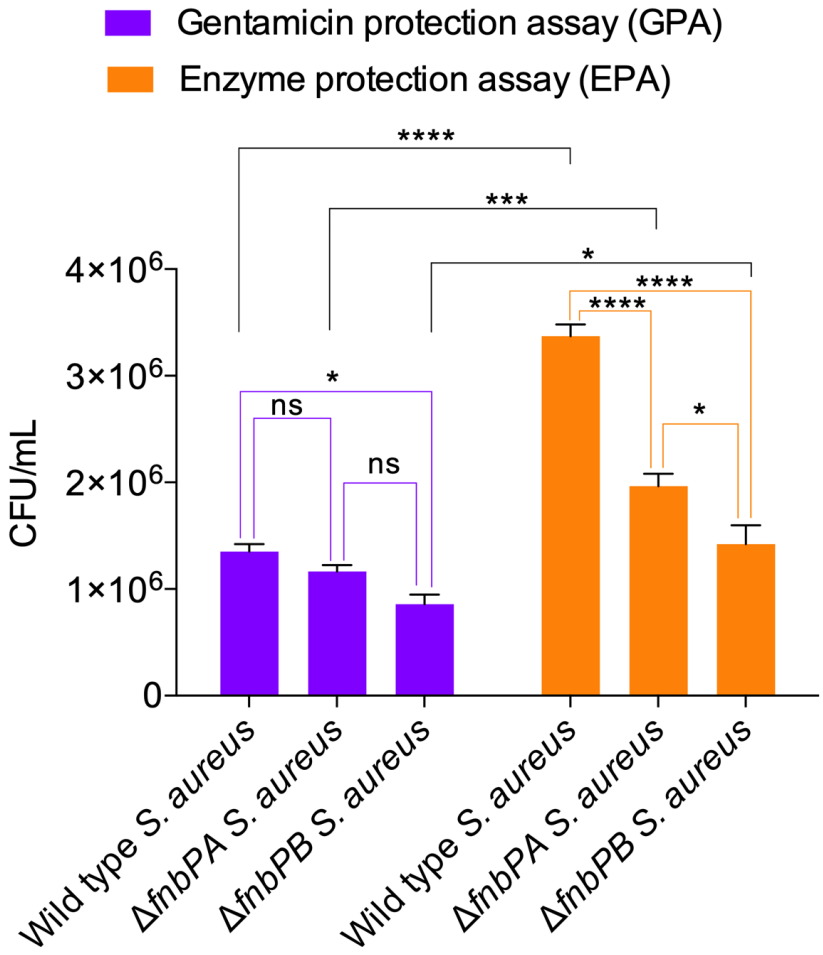

FIG S11 Comparative assessment of the invasion potentials of *S. aureus* and its isogenic mutants lacking the fibronectin binding protein FnBPA or FnBPB using GPA and EPA in phagocytic RAW264.7 cells. The reduced recovery of colony forming units during GPA indicates that the gentamicin affects the number of intracellular-survived *S. aureus* at a greater extent in phagocytic RAW264.7 cells than that of the non-phagocytic host, HEK293 cells (Fig 5A). It is known that internalization of bacteria into macrophages is not dependent on fibronectin bridging events between FnbPs and integrins. However, with the marginally reduced internalization of *fnbPs* mutants compared to wild-type *S. aureus* in mouse macrophage, RAW264.7 cells do suggest the possibility of the existence of an unknown mechanism. Internalization potentials of *S. aureus* strains in mouse macrophage, RAW264.7 cells were compared by one-way ANOVA with Bonferroni's multiple comparisons test. The p values are *, p <0.05; ***, p <0.001; and ****, p <0.0001.

FIG S12

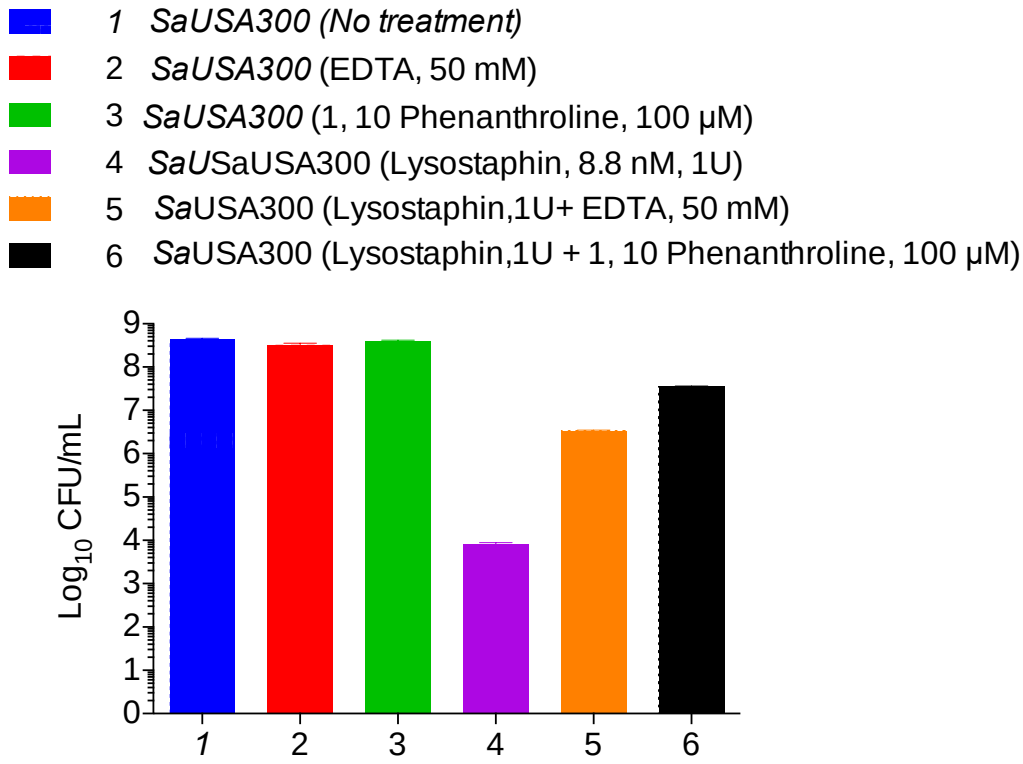

FIG S12 Tunability of lysostaphin activity. The *S. aureus* cells were harvested, washed with PBS (pH 7.4), and treated as shown in the figure labels (1-6 in X-axis). Both the general metal ion chelator (EDTA) and the zinc-specific chelator (1, 10-phenanthroline) were found to inhibit the activity of lysostaphin. However, 1, 10-phenanthroline was found to be more efficient than EDTA, as lysostaphin is a zinc-metallopeptidase (2). It is noteworthy that an assessment of the lysostaphin inhibition by measuring the *S. aureus* cell survival is extremely challenging, since it is hard to detect small changes in the number of S. *aureus* cells using lysostaphin, which shows extremely high and fast S. *aureus* killing activity.

FIG S13

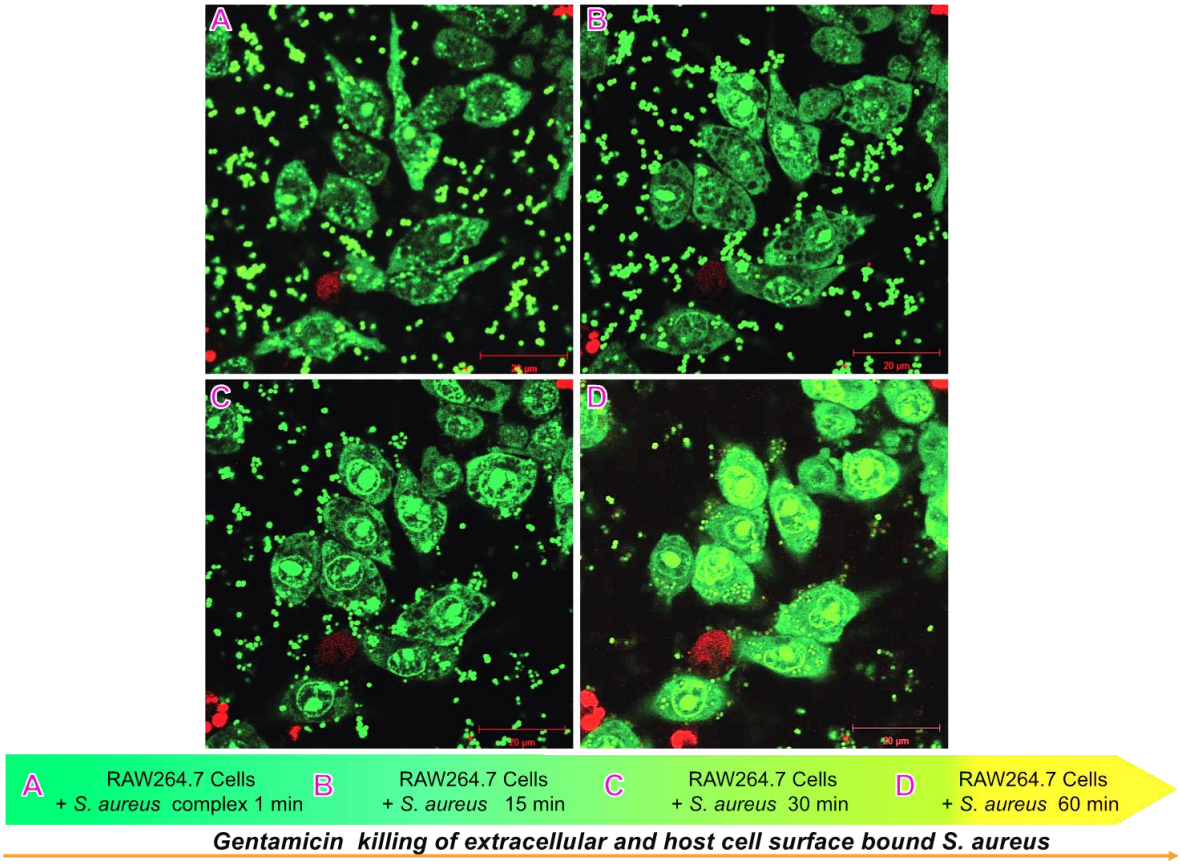

FIG S13 Snapshot of video V1 showing gentamicin-mediated killing of extracellular *S. aureus* infected into RAW264.7 cells. The representative images were adapted from the supplementary video V1 at time points (A) 1 min, (B) 15 min, (C) 30 min, and (D) 60 min after treatment with gentamicin. Despite the removal of excess bacteria after 30 min infection followed by washing, there were a significant number of adhered bacteria observed in the confocal disc. It is noteworthy that the internalized bacteria (represented by green) increased with time, suggesting that adhered remaining *S. aureus* continues to get internalized even during gentamicin killing. Therefore, internalized bacteria cannot be accurately measured using the GPA.

FIG S14

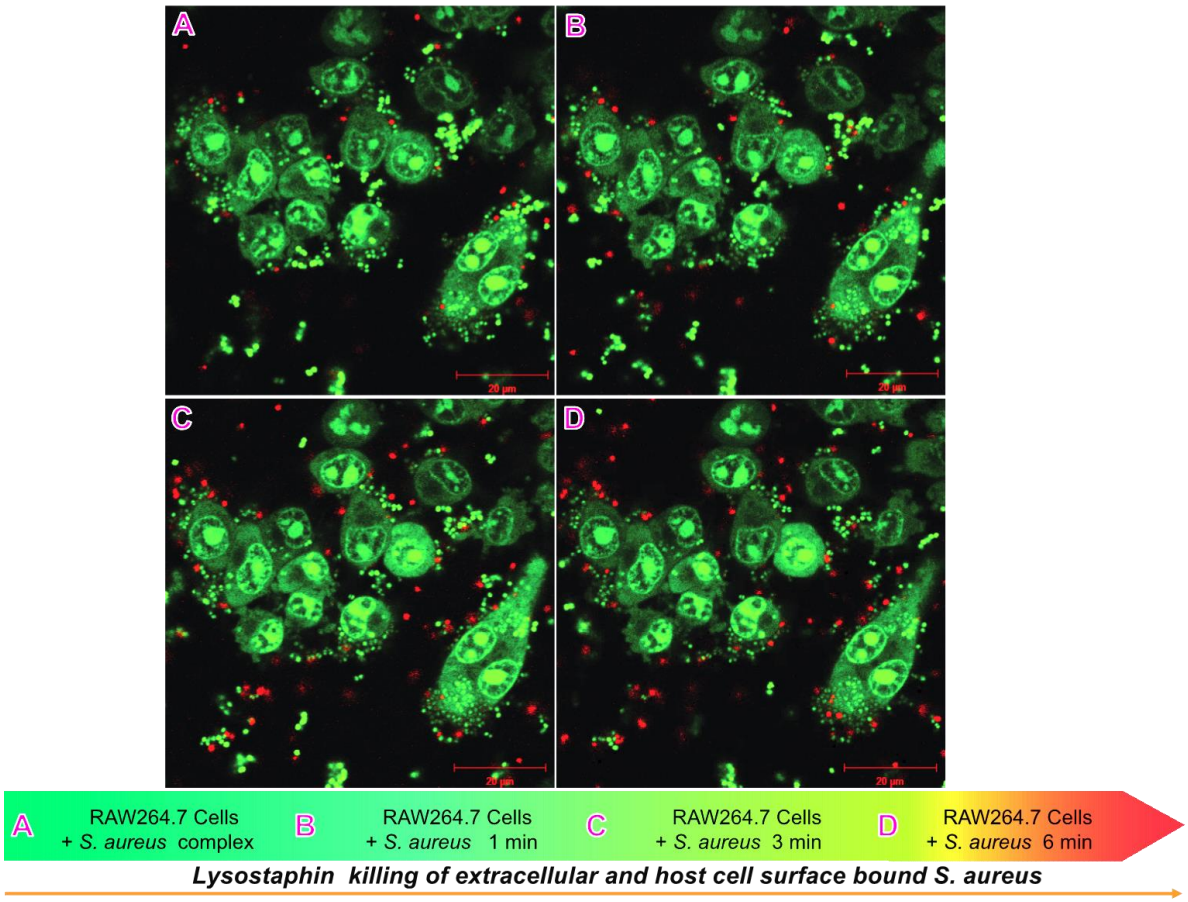

FIG S14 Snapshot of video V2 showing lysostaphin-mediated killing of extracellular *S. aureus* infected into RAW264.7 cells. The representative images were adapted from the supplementary video V2 at time points (A) 0 min, (B) 1 min, (C) 3 min, and (D) 6 min after treatment with lysostaphin. Since the lysostaphin kills the *S. aureus* within 180 second by hydrolyzing the polyglycine bridges that cross-link glycopeptide chains in the peptidoglycan of the *S. aureus* cell wall; the number of red cells increased due to dominant internalization of propidium iodide over SYTO9. Lysostaphin cannot be internalized into live host cells passively which suggests that accurate numbers of intracellular bacteria can be obtained using EPA.

B. Supplementary video legends

1. Supplementary Video V1 Visualization of the gentamicin-mediated killing of extracellular and host cell surface-attached *S. aureus* for 1 h after 30-min invasion of *S. aureus* and phagocytosis by host cells. After 30 min of infection of *S. aureus* into RAW264.7 cells, the extracellular medium was removed to eliminate excess *S. aureus*, and the host-pathogen mixture was washed twice with PBS. Then, 1 ml of fresh DMEM with 840 μM gentamicin was added to the host-pathogen mixture. The gentamicin-mediated killing was monitored for 1 h using time-lapse acquisition of images every 2 seconds (1800 images). Despite the removal of excess bacteria and washing, a significant number of *S. aureus* cells remained adhered into the confocal disc. The time-dependent monitoring of gentamicin killing demonstrated that the remaining adhered *S. aureus* cells continue to be internalized during the gentamicin killing. These results suggest that the gentamicin killing assay can confound the accurate counting of internalized bacteria. Accordingly, it is possible that the virulence potential for a pathogen and the efficacy of newly discovered antibiotics can be miscalculated when the GPA is applied.

2. Supplementary Video V2 Visualization of the lysostaphin-mediated instantaneous killing of extracellular and host cell surface-bound *S. aureus*. After 30 min of infection into RAW264.7 cells, extracellular *S. aureus* bacteria were removed by washing, and the host-pathogen mixture was treated with 2 units of lysostaphin in DMEM. The lysostaphin killing was monitored for 10 min using time-lapse acquisition of images every 2 seconds. It is noteworthy that the green fluorescence in the RAW264.7 cells (representing the internalized *S. aureus* cells) did not change during lysostaphin killing. Therefore, EPA provides a viable alternative to the GPA, both for the precise enumeration of internalized *S. aureus* and for measuring the kinetics of bacterial invasion, virulence and in the determination of efficacy of newly discovered antibacterial drugs.

C. References

1. Woiwode U, Sievers-Engler A, Lammerhofer M. 2016. Preparation of fluorescent labeled gentamicin as biological tracer and its characterization by liquid chromatography and high resolution mass spectrometry. J Pharm Biomed Anal 121:307-315.
2. Bastos MD, Coutinho BG, Coelho ML. 2010. Lysostaphin: A staphylococcal bacteriolysin with potential clinical applications. Pharmaceuticals (Basel) 3:1139-1161.